



# Dynamics of mixed lump-solitary waves of an extended (2 + 1)-dimensional shallow water wave model

Harun-Or-Roshid <sup>a,\*</sup>, Wen-Xiu Ma <sup>b,c,d,e</sup>

<sup>a</sup> Department of Mathematics, Pabna University of Science and Technology, Bangladesh

<sup>b</sup> Department of Mathematics and Statistics, University of South Florida, Tampa, FL 33620, USA

<sup>c</sup> Department of Mathematics, Zhejiang Normal University, Jinhua 321004, Zhejiang, China

<sup>d</sup> College of Mathematics and Systems Science, Shandong University of Science and Technology, Qingdao 266590, Shandong, China

<sup>e</sup> Department of Mathematical Sciences, North-West University, Mafikeng Campus, Mmabatho 2735, South Africa

## ARTICLE INFO

### Article history:

Received 12 July 2018

Received in revised form 13 September 2018

Accepted 14 September 2018

Available online 19 September 2018

Communicated by C.R. Doering

### Keywords:

Lump solution

Periodic lump wave

(2 + 1)-dimensional shallow water wave

Hirota bilinear form

## ABSTRACT

To explore the features of lump solutions, which are local in every direction of space, a (2 + 1)-dimensional extended shallow water wave model is studied, based on its bilinear representation. Several ansatzes have been utilized to determine single lump waves, lump-kink waves, single kinks and multi-lumps leading to breathers in terms of function patterns for the model. Through analyzing interactions between solitons, the impact of free parameters involved in the solutions on interaction types is exhibited. We determine a condition on the parameters under which a single kink wave can be converted into a multi-lump wave. To illustrate the interaction of exponential and periodic function waves, we show that multi-lump waves in the form of breather waves especially come into sight as a straight line or an X shape. To realize dynamics, we make various graphical analyses on the presented solutions, which gives an essential improvement in the physical realizing of higher-dimensional lump waves in oceanography and nonlinear optics.

© 2018 Elsevier B.V. All rights reserved.

## 1. Introduction

The studies of entirely integrable models are thriving as they illustrate essential features in assortment of engineering fields. Mathematicians have been investing their efforts to enlarge and affect novel procedures for solving integrable models, while physicists habitually observe dynamical behaviors of the physical systems. Various effective procedures were built in the literature to investigate and assort dynamical natures of the derived models [1–33]. It is broadly recognized that there is a substantial nonlinear effect, which is identified as that of rogue waves, arousing a vast impact in deep-ocean [1,2], nonlinear optics, plasma physics [3,4], super-fluids [5] and even in financial markets [6], etc. Tsunamis and storms-like natural effects allied with typhoons, which can be forecasted hours or a few days ago, but a rogue type lump wave episode is irregular, which is one of the underway matters in the mentioned fields of study. It is so essential to advance understanding and to smoothly supervise physical mechanisms for controlling rogue wave phenomena, in order to stifle them in the

dangerous aspects (e.g. oceanic rogue waves [19]) and to stimulate them in the helpful fields (e.g. optical rogue waves to motivate super-continuum production [3] or further valuable examples in future).

Gilson and Nimmo [8] offered lump wave solutions of the BKP equation. Imai [9] established dromion and lump wave solutions of the Ishimori-I equation. Satsuma and Ablowitz [10] presented lumps wave solution for non-linear dispersive systems. One of the authors (Ma) [11] presented a class of lump wave solutions to the (2 + 1) dimensional KP equation, and some other studies on lumps were systematically made in [23,24]. Rational solutions of the Toda lattice equation were generated in the Casoratian form in [16]. A new model namely (3 + 1)-dimensional potential-Yu-Toda-Sasa-Fukuyama (YTSF)-like equation was derived and lump wave characteristics of the model was analyzed in [21]. Hosseini et al. [22] investigated characteristics of the solitary waves and rogue waves and their interaction phenomena in a (2 + 1)-dimensional Breaking Soliton equation. Lump and rogue waves are clearly stated and physically explained in [31,33].

We consider an extended (2 + 1)-dimensional shallow water wave equation, introduced by Yu et al. [20], and written as

$$u_{yt} + 3u_{xxxx} - 3u_{xx}u_y - 3u_xu_{xy} + \kappa u_{xy} = 0, \quad (1)$$

\* Corresponding author.

E-mail address: [harunoroshidmd@gmail.com](mailto:harunoroshidmd@gmail.com) (Harun-Or-Roshid).

where  $\kappa$  is a constant. This is a nonlinear particle differential equation in two spatial and a temporal coordinate, describing the evolution of nonlinear shallow water wave propagation. Equation (1) is a frequently utilized model for exploring dynamics of solitons and nonlinear waves to describe the  $(2+1)$ -dimensional interaction of a Riemann wave propagating along the  $y$ -axis with a long wave propagating along the  $x$ -axis in fluid dynamics, plasma physics and weakly dispersive media.

Based on the Hirota bilinear method [17,18], the purpose of the present paper is to employ some efficient and straight ansatzes to determine lump wave, multi-lump wave and lump-kink wave solutions and their dynamics for the above  $(2+1)$ -dimensional extended shallow water wave equation.

## 2. Bilinear formalism

Setting  $u = -\Phi_x$ , then inserting it into Eq. (1) and integrating it with respect to  $x$  yields:

$$\Phi_{yt} + 3\Phi_{xxx} + 3\Phi_{xx}\Phi_{xy} + \kappa\Phi_{xy} - \gamma = 0, \quad (2)$$

where  $\gamma$  is a constant. ‘ $P$ -polynomial theory (see, e.g., [18]) gives  $\Phi = 2\ln\varphi$  and thus we have  $u = -2(\ln\varphi)_x$ .

All of the above can get a hold the bilinear form of Eq. (1) as

$$(D_y D_t + D_x^3 D_y + \kappa D_x D_y) \varphi \cdot \varphi - \gamma \varphi^2 = 0. \quad (3)$$

Expanding the Eq. (3) through Hirota bilinear  $D$ -operator to Hirota direct method as

$$\prod_{i=1}^M D_{x_i}^{n_i} a \cdot b = \prod_{i=1}^M \left( \frac{\partial}{\partial x_i} - \frac{\partial}{\partial x'_i} \right)^{n_i} a(x) b(x') \Big|_{x'=x}, \quad (4)$$

where  $x = (x_1, \dots, x_M)$ ,  $x' = (x'_1, \dots, x'_M)$  are vectors and  $n_1, \dots, n_M$  are random non-negative integers.

The Eq. (2) has the solution

$$u = -2(\ln\varphi)_x, \quad (5)$$

where  $\varphi(x, y, t)$  solves (3). From Eq. (4), Eq. (3) yields

$$\begin{aligned} & \varphi \varphi_{yt} - \varphi_y \varphi_t + \varphi \varphi_{xxx} - \varphi_y \varphi_{xx} + 3\varphi_{xy} \varphi_{xx} - 3\varphi_{xxy} \varphi_x \\ & + \kappa(\varphi \varphi_{xy} - \varphi_x \varphi_y) - \gamma \varphi^2 = 0. \end{aligned} \quad (6)$$

Note that  $u = -2(\ln\varphi)_x$  translates the PDE Eq. (1) to its bilinear form (3). So if  $\varphi$  is a solution of Eq. (6), then the transformation  $u = -2(\ln\varphi)_x$  will give a solution of the extended shallow water wave model Eq. (1).

## 3. Single lump solution

Now, we pay attention to ascertaining lump type solutions of the Eq. (1) as

$$\varphi = \vartheta^2 + \tau^2 + k_9, \quad (7)$$

where  $\vartheta(x, y, t) = k_1 x + k_2 y + k_3 t + k_4$ ,  $\tau(x, y, t) = k_5 x + k_6 y + k_7 t + k_8$ .

Upon inserting Eq. (7) into Eq. (6) and after some simplification, we set the coefficients of powers of the independent variables to equal to zero, and obtain a set of algebraic equations on the parameters  $k_i$ ; ( $i = 1, 2, \dots, 9$ ). Solving this set of algebraic equations for the unknown parameters  $k_i$ ; ( $i = 1, 2, \dots, 9$ ), we acquire the subsequent solution:

$$\left\{ \gamma = 0, k_1 = -\frac{k_3}{\kappa}, k_2 = \frac{\kappa k_5 k_6}{k_3}, k_7 = -\kappa k_5 \right\}. \quad (8)$$

The solution Eq. (7) with Eq. (8) for the Eq. (1) contains six free parameters  $k_3, k_4, k_5, k_6, k_8, k_9$  and gives a lump solution if the condition of  $k_3 \neq 0$  and  $k_9 > 0$  holds. This condition assured localization and analyticity of the achieved lump solution in every direction in the  $xy$ -plane. Dynamical characteristics of this wave solution depend on the free parameters. All six involved parameters are random provided that the solutions are well behaved all over the place if the condition of  $k_3 \neq 0$  and  $k_9 > 0$  holds. This rational solution is a line wave, which is distinctly different from a moving line soliton. Indeed,  $u \rightarrow 0$  for  $\vartheta$  or  $\tau \rightarrow \pm\infty$ , i.e. the solution is rhythm with algebraically decaying about  $\vartheta$  or  $\tau$ . As  $t \rightarrow \pm\infty$ , the line wave uniformly goes to a constant background; but in the intermediate time, it attains its biggest amplitude. It also exhibits a special structure rationally localized in every direction with space. The wave exhibits a pattern with one high peak and a deep hole. By virtue of the extreme value theory of functions of several variables, setting  $k_4 = k_8 = 0$  in this solution, we see that the maximum amplitude attains  $\frac{2}{\kappa} \sqrt{\frac{k_3^2 + \kappa^2 k_5^2}{k_9}}$  at  $(-\kappa \sqrt{\frac{k_9}{(k_3^2 + \kappa^2 k_5^2)}}, 0)$  and the minimum,  $-\frac{2}{\kappa} \sqrt{\frac{k_3^2 + \kappa^2 k_5^2}{k_9}}$  at  $(\kappa \sqrt{\frac{k_9}{(k_3^2 + \kappa^2 k_5^2)}}, 0)$ .

In Fig. 1(a), a single lump like rogue wave determined by the solution Eq. (7) with Eq. (8) is shown. The wave exhibits a pattern with one high peak and a deep hole hidden under the plane wave. The amplitude of the wave solution determines its facial appearance as a bright–dark lump wave, which possesses the maximum  $2\sqrt{2}$  at  $(-\frac{1}{\sqrt{2}}, 0)$  and the minimum  $-2\sqrt{2}$  at  $(\frac{1}{\sqrt{2}}, 0)$ . As a lump wave is a kind of killer wave or abnormal wave, its amplitude in the 2D plot is an important factor to study. The evolution characteristics of the lump wave at different locations are plotted in Fig. 1(b), which shows that the wave solution is symmetric about the  $y$ -axis as it coincides when  $y = -1$  and  $y = 1$ ; or  $y = -2$  and  $y = 2$ ; the maximum amplitude is exhibited in its centre  $y = 0$ . In effect, the overall mass of the lump given by  $\int_{-\infty}^{\infty} \int_{-\infty}^{\infty} u(\vartheta, \tau) d\vartheta d\tau$ , is vanishing so that the loads of masses in the upper and down hump accurately balance.

## 4. Interaction of lump waves with solitary waves

In this section, we are paying attention to interaction solutions between lump type rogue waves with a well-known kink type solitary wave solution to the extended shallow water wave equation (1). Here, we evoke a trial solution as a combination of two quadratic algebraic functions and an exponential function:

$$\varphi = \vartheta^2 + \tau^2 + k_9 + h\eta, \quad (9)$$

where  $\vartheta(x, y, t) = k_1 x + k_2 y + k_3 t + k_4$ ,  $\tau(x, y, t) = k_5 x + k_6 y + k_7 t + k_8$  and

$$\eta = \exp(\alpha_1 x + \alpha_2 y + \alpha_3 t).$$

Applying the similar process carried out in the previous section for the unknown parameters  $k_i$ ; ( $i = 1, 2, \dots, 9$ ) and  $\alpha_1, \alpha_2, \alpha_3$ , we acquire the subsequent solution:

$$\left\{ \begin{array}{l} \gamma = 0, k_1 = -\frac{k_5 k_6}{k_2}, k_3 = \frac{\kappa k_5 k_6}{k_2}, k_7 = -\kappa k_5, \\ \alpha_3 = -\alpha_1(\kappa + \alpha_1^2), \alpha_2 = 0 \end{array} \right\}. \quad (10)$$

The solution Eq. (10) with Eq. (9) of the Eq. (1) contains eight free parameters  $k_2, k_4, k_5, k_6, k_8, k_9, \alpha_1, h$ . If only the condition of  $k_2 \neq 0$ ,  $h = 0$  and  $k_9 > 0$  holds, then it exhibits just a lump wave as in the previous section. On the other hand, if the condition of  $k_2 \neq 0$ ,  $h \neq 0$  and  $k_9 > 0$  holds, then it gives a mixed or interaction

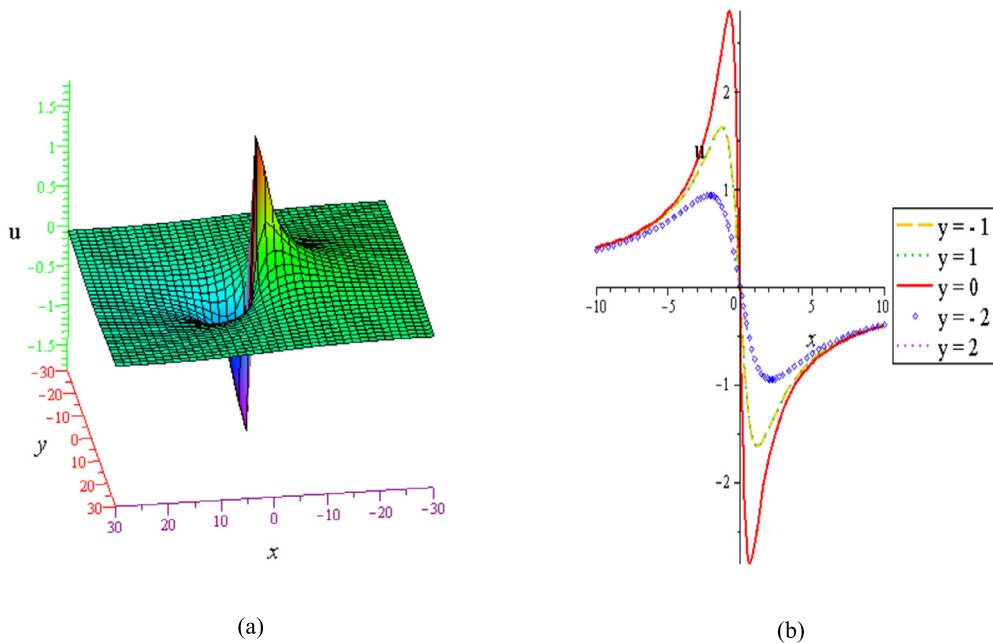


**Fig. 1.** (Color online) Perspective view of the solution Eq. (5) with Eq. (7) and constraint Eq. (8) for the parametric values  $\gamma = 0$ ,  $\kappa = k_3 = k_5 = k_6 = k_9 = 1$ ,  $k_4 = k_8 = 0$ : (a) 3D plot and (b) 2D view at  $t = 0$  for different values of  $y$ .

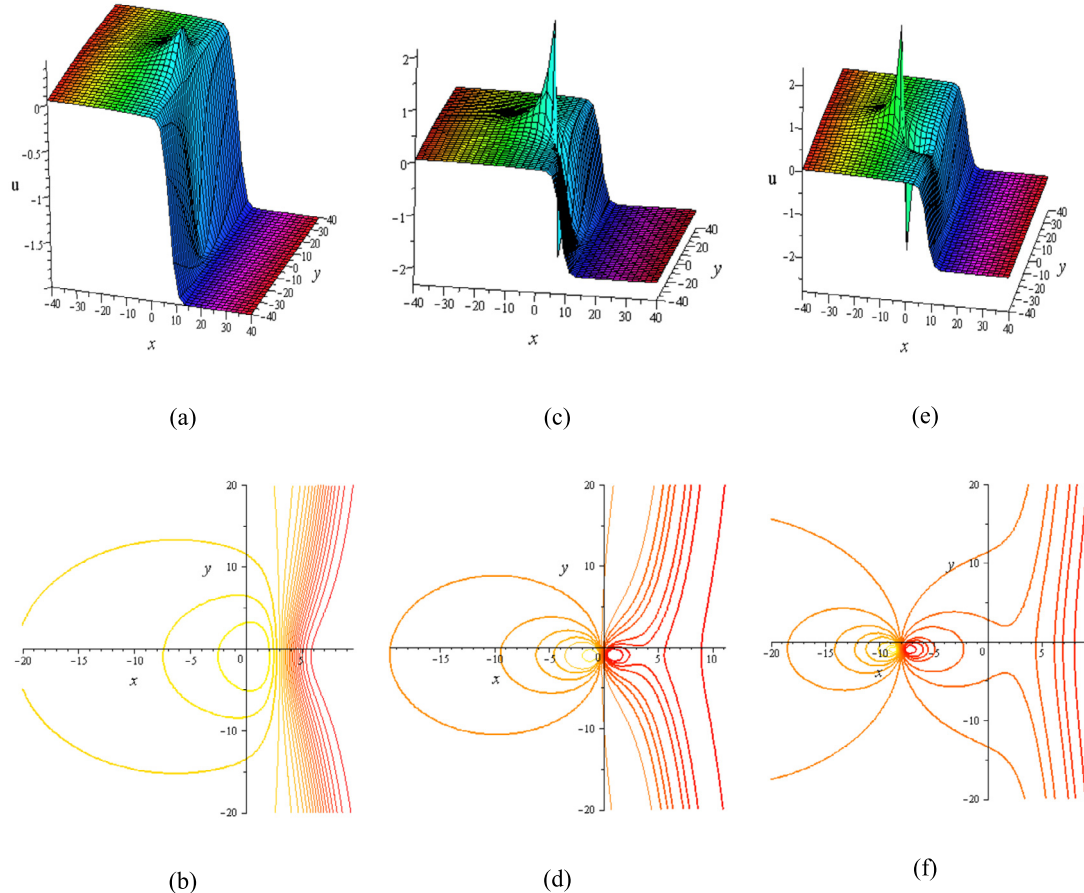


**Fig. 2.** (Color online) Perspective view of the solution Eq. (5) with Eq. (9) and Eq. (10) for the parametric values  $\kappa = -1$ ,  $k_2 = k_4 = k_5 = k_6 = k_8 = k_9 = \alpha_1 = h = 1$ ,  $\gamma = 0$ : (a) 3D plot at  $t = -8$ , (b) corresponding contour plot of (a), (c) 3D plot at  $t = 0$ , (d) corresponding contour plot of (c), (e) 3D view at  $t = 8$  and (f) corresponding contour plot of (e).

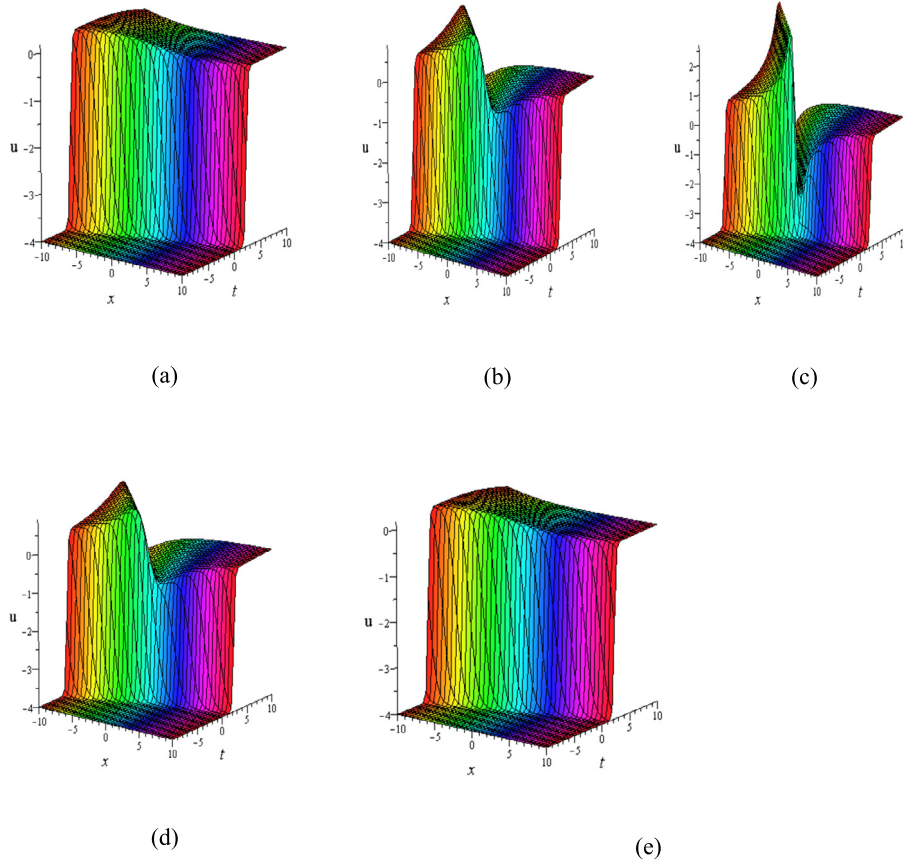


**Fig. 3.** (Color online) Perspective view of the solution Eq. (5) with Eq. (9) and Eq. (10) for the parametric values  $\kappa = k_2 = -1$ ,  $k_4 = k_5 = k_6 = k_8 = k_9 = 1$ ,  $\alpha_1 = 2$ ,  $h = 1$ ,  $\gamma = 0$ : (a) at  $y = -10$ , (b) at  $y = -2$ , (c) at  $y = 0$ , (d) at  $y = 2$  and (e) at  $y = 10$ .

of a lump wave with a kink wave. Some (see Fig. 2) 3D plots and corresponding contour plots of the achieved solution Eq. (10) with Eq. (9) are given with the demanding variety of free parameters.

As in Fig. 2, it can be clearly seen that the non-elastic lump wave starts from a constant background in the entire  $(x, y)$  plane (see Fig. 2(a) and corresponding contour plot Fig. 2(b)) and comes into interaction with the elastic kink wave in the intermediate time  $t = 0$  (see Fig. 2(c) and corresponding contour plot Fig. 2(d)). When the time increases, the lump goes away from the elastic kink (see Fig. 2(e) and corresponding contour plot Fig. 2(f)) and ultimately goes back to a constant background as  $t \rightarrow \infty$ .

On the other hand, as seen in Fig. 3, the non-elastic lump wave comes from a constant background in the  $(x, t)$  plane (see Fig. 3(a)). Gradually, the lump wave takes its bigger amplitude with an elastic kink (see Fig. 3(b)) and ultimately giants the highest/lowest amplitude at  $y = 0$  (see Fig. 3(c)). After the midway, the amplitude of the lump wave again gradually tends to diminish (see Fig. 3(d)) and finally it goes back to a constant background as seen in Fig. 3(e). But throughout the overall interaction (before, after and during interaction), the kink wave keeps its shape, size and constant speed, and displays its elastic situation.

## 5. Multi-lump wave solutions

In this section, we are paying attention to determination of multi-lump wave solutions from collisions between exponential and trigonometric functions to the extended shallow water wave model (1).

**Case-1:** Here, we evoke a trial solution as a combination of two exponential functions and a sinusoidal periodic function:

$$\begin{aligned} \varphi &= \exp(-\rho_1(x + n_1 y - \omega_1 t)) + h_1 \exp(\rho_1(x + n_1 y - \omega_1 t)) \\ &\quad + h_2 \sin(\rho_2(x + n_2 y - \omega_2 t)) \\ &= 2\sqrt{h_1} \cosh\{\rho_1(x + n_1 y - \omega_1 t) + \ln(\sqrt{h_1})\} \\ &\quad + h_2 \sin(\rho_2(x + n_2 y - \omega_2 t)), h_1 > 0. \end{aligned} \quad (11)$$

Inserting Eq. (11) with Eq. (5) into Eq. (6) and setting all the coefficients of dissimilar powers of  $\exp$ ,  $\sin$ ,  $\cos$  and their product to zero, we gain a system of polynomial equations. Solving this system of equations for the unknown parameters  $\rho_i, n_i, \omega_i, h_i$ ;  $(i = 1, 2)$ , we get hold of the subsequent solutions:

$$\left\{ \gamma = 0, \rho_1 = \frac{\sqrt{-\kappa}}{2}, \rho_2 = \frac{\sqrt{\kappa}}{2}, h_1 = \frac{h_2^2}{4}, n_1 = n_2, \omega_1 = \omega_2 \right\}, \quad (12)$$

$$\left\{ \gamma = 0, \rho_2 = \pm \sqrt{\frac{\kappa}{2} + \rho_1^2}, h_1 = -\frac{n_2 h_2^2 (\kappa + 2\rho_1^2)}{8n_1 \rho_1^2}, \right. \\ \left. \omega_2 = -\omega_1, \omega_1 = -(\kappa/2 + 2\rho_1^2) \right\}. \quad (13)$$

In Fig. 4, the solution Eq. (5) with Eq. (11) and the constraints in Eq. (12) of the Eq. (1), exhibits a periodic lump type pulsate wave propagation, coming in terms of complex functions, and gives an interaction of periodic multi-lump waves with different small amplitudes. Pulses are given in very quick times.

As depicted in Fig. 5, the solution Eq. (5) with Eq. (11) and the constraints in Eq. (13) of the Eq. (1), gives collisions between two exponential solitons with a sinusoidal function, viewed in periodically multi-lump propagations along a straight line with a certain angle with the  $t$ -axis and  $x$ -axis. Its speed, tallness and thickness remain the same all over the propagation. Fig. 5(a) shows a 3D profile of the interaction, in which some lumps periodically get

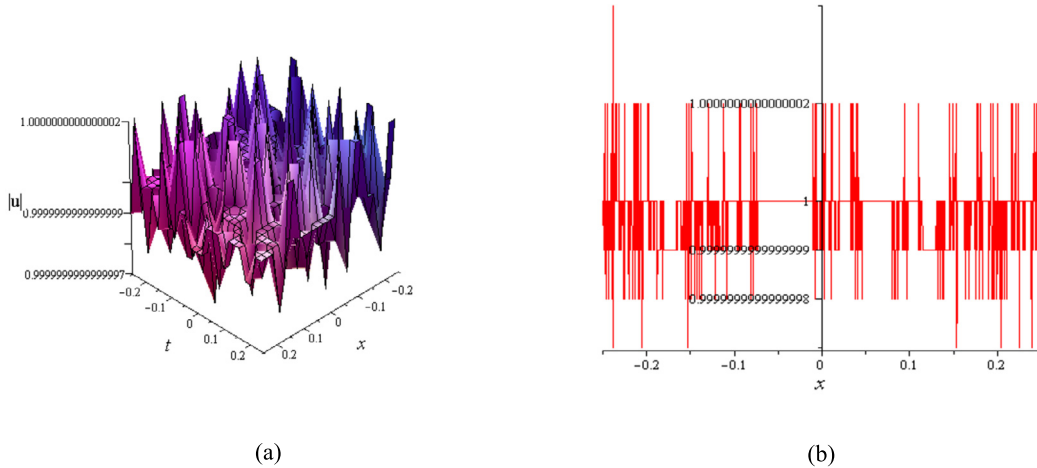


**Fig. 4.** (Color online) Perspective view of the solution Eq. (5) with Eq. (11) and constraint Eq. (12) for  $\kappa = -1$ ,  $n_1 = n_2 = 2$ ,  $h_2 = \omega_1 = \omega_2 = 1$  along  $y = 0$ : (a) 3D plot (left) and (b) 2D plot (right) at  $t = 1$ .

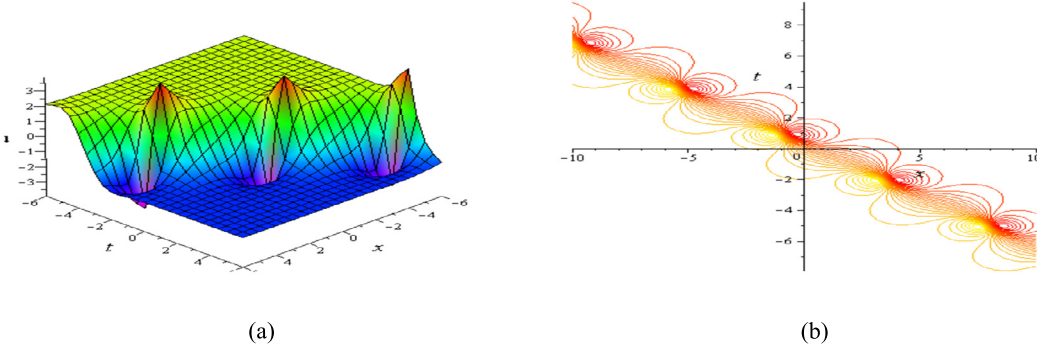


**Fig. 5.** (Color online) Perspective view of the solution Eq. (5) with Eq. (11) and constraint Eq. (13) for  $\kappa = -1$ ,  $n_1 = \rho_1 = h_2 = 1$ ,  $n_2 = -3$  along  $y = 0$ : (a) 3D plot (left) and (b) corresponding contour plot (right).

into a kink wave, being at equal distance from each other. The equidistance and the same angle are clearly observed from its corresponding contour plot in the Fig. 5(b). Moreover, we see that the solution is not only a space periodic breather wave but also a time periodic breather wave.

**Case-2:** In this case, we take a trial solution as a combination of two exponential functions and a sinusoidal periodic function:

$$\begin{aligned} \varphi = & \exp(-\rho_1(x + n_1 y - \omega t)) + h_1 \exp(\rho_1(x + n_1 y - \omega t)) \\ & + h_2 \cos(\rho_2(x + n_2 y - \omega t)) \\ = & 2\sqrt{h_1} \cosh\{\rho_1(x + n_1 y - \omega t) + \ln(\sqrt{h_1})\} \\ & + h_2 \cos(\rho_2(x + n_2 y - \omega t)), h_1 > 0. \end{aligned} \quad (14)$$

Upon substituting Eq. (14) with Eq. (5) into the bilinear form Eq. (6) and then after some simplification, through the computer software Maple 13, we set all coefficients of  $\exp$ ,  $\sin$ ,  $\cos$  and their product to zero, and obtain a set of polynomial equations in terms of the unknown parameters  $\rho_1$ ,  $\rho_2$ ,  $n_1$ ,  $n_2$ ,  $\omega$ ,  $h_1$  and  $h_2$ . Solving this system of equations for the unknown parameters, we achieve

$$\begin{cases} \rho_2 = \frac{n_1 \rho_1 \sqrt{-1}}{n_2}, \omega = \frac{\rho_1^2 n_1 (n_1 + 2n_2) + n_2^2 (\kappa + \rho_1^2)}{n_2^2}, \\ h_1 = \frac{h_2^2 n_1 (3n_1 + n_2)}{4n_2 (n_1 + 3n_2)} \end{cases}, \quad (15)$$

where  $\rho_1$ ,  $n_1$ ,  $n_2$ ,  $h_2$  are arbitrary constants.

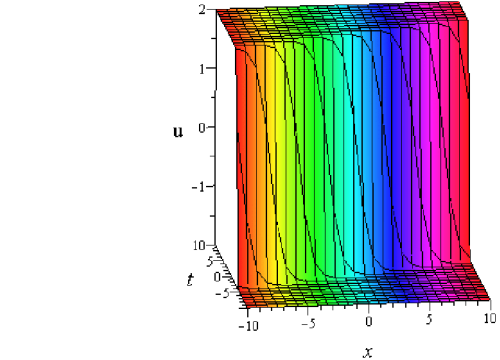


**Fig. 6.** (Color online) Perspective view of the solution Eq. (5) with Eq. (14) and constraint Eq. (15) for  $\kappa = -1$ ,  $n_1 = n_2 = \rho_1 = h_2 = 1$ ,  $\gamma = 0$  along  $y = 0$ .

In the subsequent, Fig. 6 presents a kink soliton solution Eq. (5) with Eq. (14) and the constraints in Eq. (15) of the Eq. (1) as a combination of two kinks coming from a two  $\cosh$  soliton, since the parameter  $\rho_2$  gives a complex value (see the constraint in Eq. (15)) i.e., two exponential functions make a  $\cosh$  soliton and the complex  $\rho_2$  reduces the  $\cos$  function to a  $\cosh$  soliton. Interesting phenomena can be gathered by keeping the  $\cos$  function to its own form. To do that, we should take  $n_1 = \sqrt{-1}$  to reduce  $\rho_2$  to a real parameter and keep the  $\cos$  function to its own form. This makes a collision between two exponential solitons with a periodic cosine function, viewed in periodically multi-lump propagations along two cross straight lines (i.e., an X-shape soliton solution) with a certain angle with the  $t$ -axis and the  $x$ -axis. Its

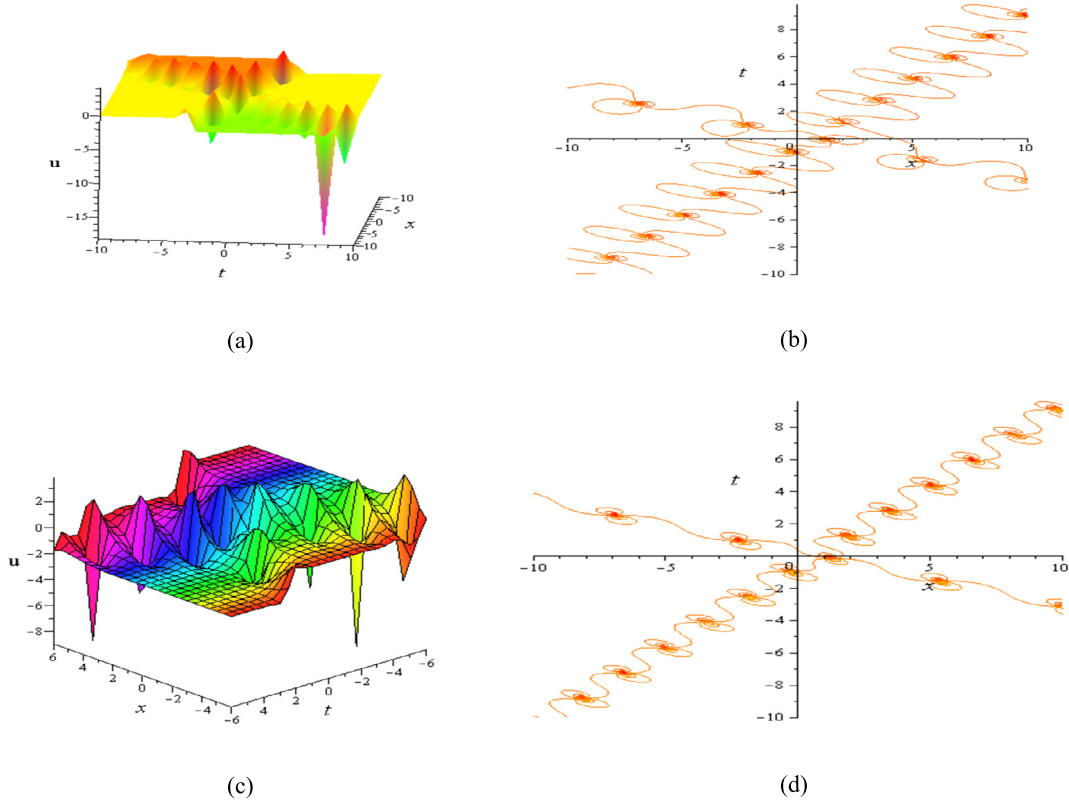


**Fig. 7.** (Color online) Perspective view of the solution Eq. (5) with Eq. (14) and constraint Eq. (15) for  $\kappa = -1$ ,  $n_1 = \sqrt{-1}$ ,  $n_2 = \rho_1 = h_2 = 1$ ,  $\gamma = 0$  along  $y = 0$ : (a) 3D plot of real part and (b) corresponding contour plot of the real part; (c) 3D plot of imaginary part and (b) corresponding contour plot of the imaginary part.

speed, tallness and thickness remain the same all over the propagation. Fig. 7(a, c) shows a 3D profile of the interaction, in which some lumps periodically get into a kink wave, being at equal distance from each other. The equidistance and the same angle are clearly observed from its corresponding contour plot in the Fig. 7(b, d). Moreover, we see that the solution is not only the space periodic breather wave but also the time periodic breather wave.

## 6. Conclusion

In conclusion, the  $(2+1)$  dimensional extended shallow water wave model has been systematically analyzed. Various productive ansatzes have been utilized to determine single lump waves, lump-kink waves, single kink waves and multi-lump waves with different function patterns for the model, based on its Hirota bilinear form. We have analyzed the results in details and shown that the simple lump waves are line local waves, which occur from a constant background with a line sketch and retract back to it again. The result also shows that lump waves can come from an extreme behavior of breather waves in high dimensions. It is worthy of mentioning that such studies recently attract much attention and can be facilitated to enrich dynamical properties of nonlinear shallow water wave fields.

Moreover, there are some other interesting studies on algebro-geometric solutions (see, e.g., [25,26]) and interaction solutions for a few integrable equations in  $(2+1)$ -dimensions (see, e.g., [27,28] for lump-kink interaction solutions and [29–33] for lump-soliton interaction solutions). One of the particularly interesting questions for us is whether one can carry out reductions of the algebro-geometric solutions to get lump or lump-kink and lump-soliton solutions.

## References

- [1] P. Müller, C. Garrett, A. Osborne, Rogue waves, *Oceanography* 18 (2005) 66–75.
- [2] C. Kharif, E. Pelinovsky, A. Slunyaev, *Rogue Waves in the Ocean*, Advances in Geophysical and Environmental Mechanics and Mathematics, Springer-Verlag, Berlin, 2009.
- [3] D.R. Solli, C. Ropers, P. Koonath, B. Jalali, Optical rogue waves, *Nature* 450 (2007) 1054–1057.
- [4] N. Akhmediev, J.M. Dudley, D.R. Solli, S.K. Turitsyn, Recent progress in investigating optical rogue waves, *J. Opt.* 15 (2013) 060201.
- [5] A.N. Ganshin, V.B. Efmov, G.V. Kolmakov, L.P. Mezhov-Deglin, P.V.E. McClintock, Observation of an inverse energy cascade in developed acoustic turbulence in superfluid helium, *Phys. Rev. Lett.* 101 (2008) 065303.
- [6] V.B. Matveev, Generalized Wronskian formula for solutions of the KdV equations: first applications, *Phys. Lett. A* 166 (3–4) (2002) 205–208.
- [7] W.X. Ma, Complexiton solutions to the Korteweg-de Vries equation, *Phys. Lett. A* 301 (1–2) (2002) 35–44.
- [8] C.R. Gilson, J.J.C. Nimmo, Lump solutions of the BKP equation, *Phys. Lett. A* 147 (8–9) (1990) 472–476.
- [9] K. Imai, Dromion and lump solutions of the Ishimori-I equation, *Prog. Theor. Phys.* 98 (5) (1997) 1013–1023.
- [10] J. Satsuma, M.J. Ablowitz, Two-dimensional lumps in non-linear dispersive systems, *J. Math. Phys.* 20 (7) (1979) 1496–1503.
- [11] W.X. Ma, Lump solutions to the Kadomtsev-Petviashvili equation, *Phys. Lett. A* 379 (36) (2015) 1975–1978.
- [12] S.J. Yu, K. Toda, N. Sasa, T. Fukuyama,  $N$  soliton solutions to the Bogoyavlenskii-Schiff equation and a quest for the soliton solution in  $(3+1)$  dimensions, *J. Phys. A* 31 (14) (1998) 3337–3347.
- [13] H.O. Roshid, M.A. Akbar, M.N. Alam, M.F. Hoque, N. Rahman, New extended  $(G'/G)$ -expansion method to solve nonlinear evolution equation: the  $(3+1)$ -dimensional potential-YTSF equation, *SpringerPlus* 3 (2014) 122.
- [14] M.A. Noor, S.T. Mohyud-Din, A.W. Eisa, A. Al-Said, Exp-function method for traveling wave solutions of nonlinear evolution equations, *Appl. Math. Comput.* 216 (2010) 477–483.
- [15] S.T. Mohyud-Din, E. Negahdary, M. Usman, A meshless numerical solution of the family of generalized fifth-order Korteweg-de Vries equations I, *Int. J. Numer. Methods Heat Fluid Flow* 22 (5) (2012) 641–658.
- [16] W.X. Ma, Y. You, Rational solutions of the Toda lattice equation in Casoratian form, *Chaos Solitons Fractals* 22 (2004) 395–406.

- [17] C. Gilson, F. Lambert, J. Nimmo, R. Willox, On the combinatorics of the Hirota D-operators, *Proc. R. Soc. Lond. A* 452 (1996) 223–234.
- [18] W.X. Ma, Bilinear equations, Bell polynomials and linear superposition principle, *J. Phys. Conf. Ser.* 411 (2013) 012021.
- [19] K. Dysthe, H.E. Krogstad, P. Müller, Oceanic rogue waves, *Annu. Rev. Fluid Mech.* 40 (2008) 287.
- [20] H.H. Dong, Y.F. Zhang, Exact periodic wave solution of extended (2+1)-dimensional shallow water wave equation with generalized  $D_{\bar{p}}$ -operators, *Commun. Theor. Phys.* 63 (2015) 401–405.
- [21] H.O. Roshid, Lump solutions to a (3+1)-dimensional potential-Yu-Toda-Sasa-Fukuyama (YTSF) like equation, *Int. J. Appl. Comput. Math.* 3 (2017) 1455.
- [22] M.B. Hossen, H.O. Roshid, M.Z. Ali, Characteristics of the solitary waves and rogue waves with interaction phenomena in a (2+1)-dimensional Breaking Soliton equation, *Phys. Lett. A* 382 (2018) 1268–1274.
- [23] W.X. Ma, Y. Zhou, Lump solutions to nonlinear partial differential equations via Hirota bilinear forms, *J. Differ. Equ.* 264 (2018) 2633–2659.
- [24] S.T. Chen, W.X. Ma, Lump solutions to a generalized Bogoyavlensky-Konopelchenko equation, *Front. Math. China* 13 (3) (2018) 525–534.
- [25] W.X. Ma, Trigon al curves and applications to algebro-geometric solutions I, *Proc. R. Soc. A* 473 (2017) 20170232.
- [26] W.X. Ma, Trigon al curves and applications to algebro-geometric solutions II, *Proc. R. Soc. A* 473 (2017) 20170233.
- [27] H.Q. Zhao, W.X. Ma, Mixed lump-kink solutions to the KP equation, *Comput. Math. Appl.* 74 (2017) 1399–1405.
- [28] J.B. Zhang, W.X. Ma, Mixed lump-kink solutions to the BKP equation, *Comput. Math. Appl.* 74 (2017) 591–596.
- [29] W.X. Ma, X.L. Yong, H.Q. Zhang, Diversity of interaction solutions to the (2+1)-dimensional Ito equation, *Comput. Math. Appl.* 75 (2018) 289–295.
- [30] J.Y. Yang, W.X. Ma, Z.Y. Qin, Lump and lump-soliton solutions to the (2+1)-dimensional Ito equation, *Anal. Math. Phys.* (2017), <https://doi.org/10.1007/s13324-017-0181-9>.
- [31] J. Wei, X. Wang, X. Geng, Periodic and rational solutions of the reduced Maxwell-Bloch equations, *Commun. Nonlinear Sci. Numer. Simul.* 59 (2018) 1–14.
- [32] X. Wang, C. Liu, L. Wang, Rogue waves and W-shaped solitons in the multiple self-induced transparency system, *Chaos* 27 (2017) 093106.
- [33] X. Wang, C. Liu, L. Wang, Darboux transformation and rogue wave solutions for the variable-coefficients coupled Hirota equations, *J. Math. Anal. Appl.* 449 (2017) 1534–1552, <https://doi.org/10.1016/j.jmaa.2016.12.079>.